

First Charm Baryon Physics from SELEX(E781)

Fernanda G. Garcia

Departamento de Física, Universidade de São Paulo, USP, São Paulo, S.P., Brasil

Soon Yung Jun

Carnegie Mellon University, Pittsburgh, PA 15213

(For the SELEX Collaboration¹)

We present preliminary results on various aspects of charm baryon studies at the 1996-1997 fixed target experiment of Fermilab studying charm produced from incident Σ^- , proton, and π^- beams at 600 GeV. First results include the comparison of hadroproduction asymmetries for Λ_c^+ production from the 3 beams as well x_F distributions and the first observation of the Cabibbo-suppressed decay $\Xi_c^+ \rightarrow pK^-\pi^+$. The relative branching fraction of the Cabibbo-suppressed mode to the 3-body Cabibbo-favored modes is also presented.

I. INTRODUCTION

The hadroproduction of the particles with open charm is a rich area to explore the hadronization process of heavy quarks. In hadronic interactions, it is especially interesting to compare the forward production characteristics of a given charm particle species for different beam hadrons. The hadronization process may introduce a distinction between those charm hadrons which have a valence quark or anti-quark in common with the beam compared to those which do not. We assume that charm production can be factorized into perturbative and non-perturbative elements. The first part describes the production of the pair $c\bar{c}$ which the gg fusion mechanism is the main diagram. This is calculable in perturbative QCD (pQCD), which does not predict any asymmetry between the c and the \bar{c} produced. Next-to-leading order pQCD calculations introduce a small asymmetry in the quark momenta [2,3]. The soft part, or hadronization, describes the process by which charmed quarks appear as hadrons in the final state. Only phenomenological models exist at this stage. For π^- beams a large asymmetry has been observed experimentally [4,5]. We present here preliminary results for charm-anticharm asymmetries for Λ_c^+ production from three different beams.

Charm decays are also important laboratories for understanding pQCD at the charm mass scale. State-of-the-art methods for calculating non-leptonic decay rates of the charmed hadrons employ heavy quark effective theory and the factorization approximation [6]. Nonetheless, the three-body Cabibbo-suppressed decays of charmed baryons are prohibitively difficult to calculate. Measurements of relative branching fraction between simple charmed baryon states, both Cabibbo-favored and Cabibbo-suppressed, give additional insight into the structure of the decay amplitude and the validity of the factorization approximation. Until now the only Cabibbo-suppressed charmed baryon decay reported with significant statistics is $\Lambda_c^+ \rightarrow pK^-K^+$ and its resonant state, $\Lambda_c^+ \rightarrow p\phi$ [7,8]. In this paper, we report the first observation of the Cabibbo-suppressed $\Xi_c^+ \rightarrow pK^-\pi^+$ and determine the branching fraction of this decay relative to the Cabibbo-favored $\Xi_c^+ \rightarrow \Sigma^+K^-\pi^+$ mode.

II. THE SELEX EXPERIMENT

SELEX is a high energy hadroproduction experiment at Fermilab using a multi-stage spectrometer designed for high acceptance for forward interactions ($x_F = 2p_{||}/\sqrt{s} > 0.1$). The experiment aimed especially to understand charm production in the forward hemisphere and to study charmed baryon decays. Using both a negative hyperon beam (50% Σ^- , 50% π^-) and a proton beam (92% p, 8% π^+), SELEX took 15.2 billion interaction events during the 1996-1997 fix target run, tagging 600 GeV Σ^- , π^- and 540 GeV p beams with a beam TRD. The data were accumulated using a segmented charm target (5 foils: 2 Cu, 3 C, each separated by 1.5 cm) whose total thickness was 5% of interaction length for protons.

The spectrometer had silicon strip detectors to measure beam and outgoing tracks and provided precision primary and secondary vertex reconstruction. Transverse position resolution was $4\text{ }\mu\text{m}$ for the 600 GeV beam and the average longitudinal vertex position resolution was $270\text{ }\mu\text{m}$ for primary and $560\text{ }\mu\text{m}$ for secondaries, respectively. Track momenta were measured after magnetic deflection by a system of proportional wire chambers (PWC), drift chambers and silicon strip detectors. Track momentum resolution for a typical 100 GeV track was $\Delta p/p \approx 0.5\%$. The absolute momentum scale was calibrated to the K_s^0 mass. For $D^0 \rightarrow K^-\pi^+$ decays the average mass resolution was 9 MeV for D^0 momenta from 100-450 GeV. Charged particle identification was done with the Ring Image Čerenkov Radiation (RICH) detector [9] which distinguished K^\pm from π^\pm up to 165 GeV. The proton identification efficiency was greater than 95% above proton threshold ($\approx 90\text{ GeV}$) and the pion mis-identification probability was about 4%.

Interactions were selected by a scintillator trigger and an online software filter. The charm trigger required at least 4 charged tracks and 2 hits in a scintillator hodoscope after the second analyzing magnet. We triggered on about 1/3 of all inelastic interactions. Based on downstream tracking with particle identification information, the online filter selected events that had evidence for a secondary vertex among tracks completely reconstructed using the forward PWC spectrometer and the vertex silicon. This filter reduced the data size by a factor of nearly 8 at a cost of about a factor of 2 in charm written to tape as normalized from a study of unfiltered K_s^0 and Λ^0 decays. Most of the charm loss came from selection cuts that were independent of charm species or kinematic variables and which improved the signal/noise in the final sample.

The charm events were selected by the following requirements; (1) fits for both primary and secondary vertex have $\chi^2/dof < 5$, (2) Longitudinal separation L between primary and secondary vertices is greater than 8 times the combined longitudinal error σ , and (3) the reconstructed momentum vector from the secondary vertex points back to the primary vertex with good quality χ^2 , and (4) $\mathcal{L}(K)/\mathcal{L}(\pi) > 1$ for K identification and $\mathcal{L}(p)/\mathcal{L}(\pi) > 1$ for p identification, where \mathcal{L} is the likelihood function based on RICH information. Additional cuts will be explicitly described if applied.

III. CHARM HADROPRODUCTION

The production properties of charm quarks require measurements of charm hadrons. pQCD calculations can be probed experimentally using measurements of single-charm-particle inclusive distributions as a function of x_F and asymmetries, either integrated or as a function of x_F .

Previous charm hadroproduction experiments showed evidence of a large enhancement in the forward production of charmed particles that contain a quark or an antiquark in common with the beam (*leading particles*) over those that do not (*non-leading particles*), in the meson sector. Recently, this study has been extended to the production of baryons by a Σ^- beam [10].

According to our simulations and our measurements of K_s^0 decays, the SELEX spectrometer acceptance is charge independent and we have a smooth, generally constant acceptance as a function of x_F for $x_F > 0.3$. We show in Fig. 1 the integrated charm production asymmetry for $\bar{\Lambda}_c^-/\Lambda_c^+$ and D^-/D^+ for Σ^- , π^- and proton beams in the kinematic region $x_F > 0.3$.

The raw asymmetry for charm baryons is much stronger than for charm mesons in this forward x_F region for all 3 beam types. The effect is even more pronounced when the charm baryons are produced by a baryon beam. One typical explanation of this observed asymmetry is that longitudinal momentum is added to the produced charm quark if it recombines with a valence quark from the incoming particle, forming the leading particle shown in Fig. 2. This is incorporated, for example, in the Pythia simulation program [11], where the effect is overestimated for typical model parameters [5]. With this scenario in mind, we expect to find a harder x_F spectrum for leading particles than non-leading particles.

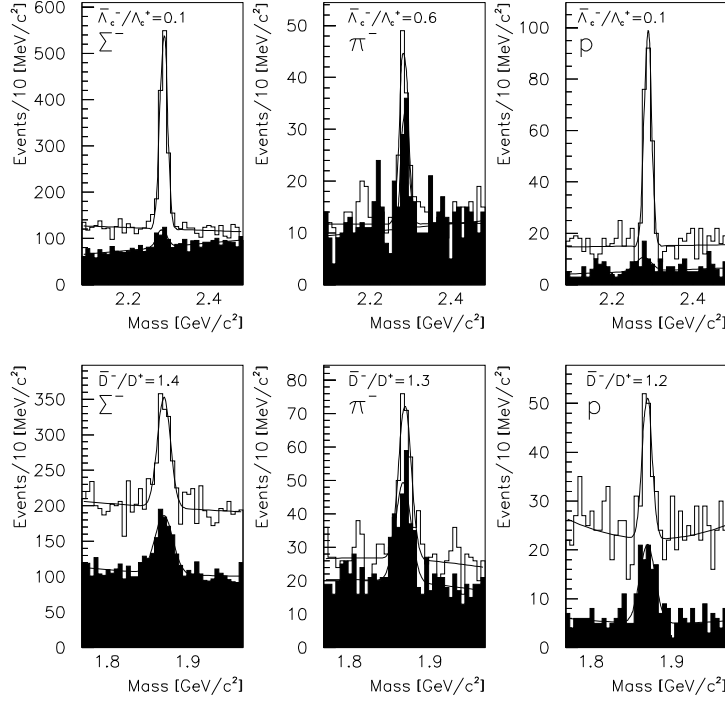


FIG. 1. $\Lambda_c^+ \rightarrow pK^-\pi^+$ and $D^+ \rightarrow K^-\pi^+\pi^+$ signal for $x_F > 0.3$ for Σ^- , π^- and proton beams.

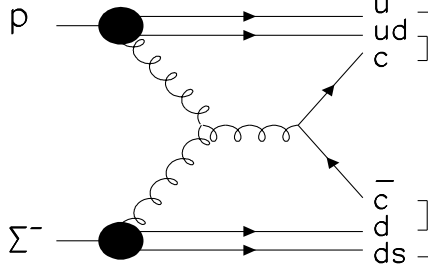


FIG. 2. An example of $gg \rightarrow c\bar{c}$ fusion production mechanism in a $p\Sigma^-$ collision. The proton remnants are represented by a quark and a diquark.

The x_F dependence of the corrected number of events from each beam is shown in figure 3. The curves are fits of the standard parametrization $(1 - x_F)^n$ to the data. The x_F distributions for Λ_c^+ show an x_F dependence for all three beam types that is harder than that reported for D mesons from a π beam. [5]. The Λ_c^+ is a leading particle for each of the three beam particles reported here, and the values of n are all consistent. Further insight into the mechanism will come from comparisons of charm meson production characteristics from these three beam hadrons. That work is in process.

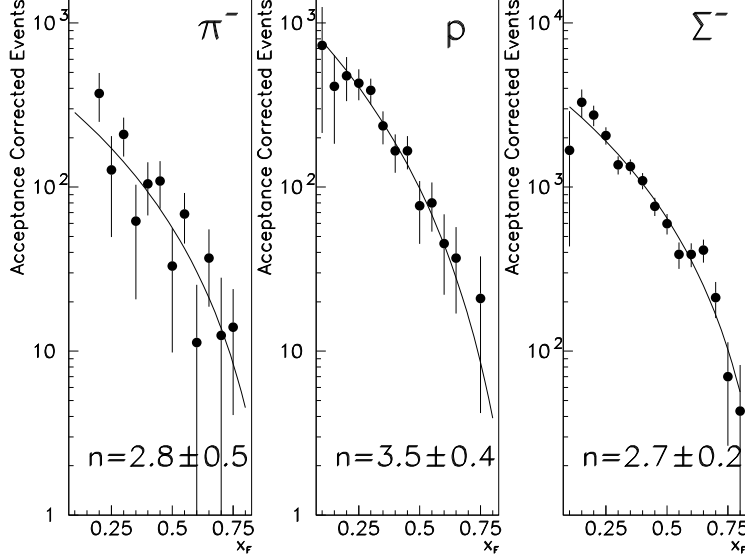


FIG. 3. $\Lambda_c^+ \rightarrow pK^-\pi^+$ production as a function of x_F for π^- , proton and Σ^- beams.

IV. CHARM BARYON Ξ_c^+ DECAYS

The study of Cabibbo-suppressed charm decays can provide useful insights into the weak interaction mechanism for non-leptonic decays [12]. The observed final state may arise either from direct quark mixing at the decay stage or, in some cases, from quark rearrangement in final-state scattering. By comparing the strengths of Cabibbo-suppressed decays to their Cabibbo-favored analogs, one can, in a systematic way, assess the contributions of the various mechanisms.

Fig. 4 shows a simple spectator diagram with external W -emission for Ξ_c^+ decaying into a Cabibbo-allowed and a Cabibbo-suppressed mode. The other Cabibbo-allowed Ξ^- mode interchanges s and d quark lines and produces a $d\bar{d}$ pair from the vacuum instead of a $d\bar{u}$ pair.

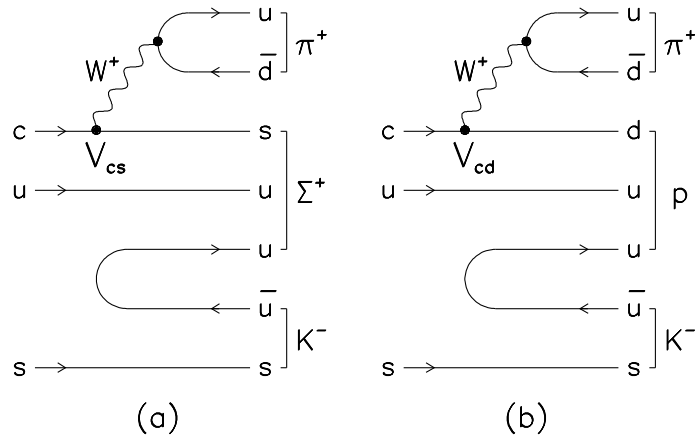


FIG. 4. An example of a spectator diagram with external W -emission for Ξ_c^+ Decays, (a) Cabibbo-favored $\Sigma^+ K^- \pi^+$ and (b) Cabibbo-suppressed $pK^-\pi^+$.

Since the decay process is similar in the two modes except flavor changing through the Cabibbo–Kobayashi–Maskawa matrix element (V_{cs} vs. V_{cd}), we expect $B(\Xi_c^+ \rightarrow pK^-\pi^+)/B(\Xi_c^+ \rightarrow \Sigma^+K^-\pi^+) = \alpha \times \tan^2\theta_c$, where θ_c is the Cabibbo angle and α is a coefficient of order one containing information about differences in the two decay mechanisms over the allowed phase space. To the extent that the relative branching ratio is different from this, we may argue for enhancement or suppression of one of the two modes.

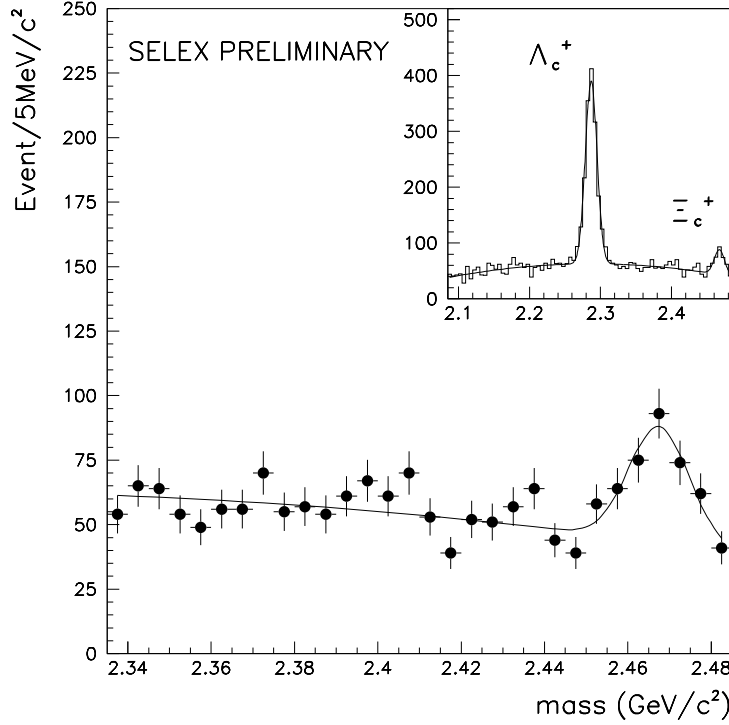


FIG. 5. The invariant mass distribution of $pK^-\pi^+$.

Fig. 5 shows the first observation of the Cabibbo-suppressed $\Xi_c^+ \rightarrow pK^-\pi^+$ decay mode. The inset of the figure shows the invariant mass distribution from reconstructed $pK^-\pi^+$ candidates with $p_\pi > 5$ GeV and the sum of transverse momentum square (Σp_T^2) of decaying particles greater than 0.3 $(\text{GeV})^2$. The large peak is the charm baryon decay, $\Lambda_c^+ \rightarrow pK^-\pi^+$ and the bump in the right corner shows the Cabibbo-suppressed $\Xi_c^+ \rightarrow pK^-\pi^+$ decay. The analysis cuts off because of a maximum mass cut in the analysis of this mode during this first pass through the data. We observed 162 ± 31 events for $\Xi_c^+ \rightarrow pK^-\pi^+$ with the Ξ_c^+ mass at (2467.4 ± 1.4) MeV. The statistical significance for the signal, $S/\sqrt{S+B}$, is (7.0 ± 1.3) in which S is the number of signal events and B is the number of background events under the signal region.

In this first reconstruction pass, hyperons (Σ^\pm, Ξ^-) were identified only inclusively in the limited decay interval ($5\text{m} < z_{\text{decay}} < 12\text{m}$). The hyperon candidate track was identified with a track having $p > 40$ GeV for which no reconstructed track segments were observed in the 14 chambers along the trajectory after the second analyzing magnet. This category of tracks (kinks by disappearance) had a unique Σ^+ identification for positive kinks but had an ambiguity for negative kinks between Σ^- and Ξ^- . Reflections in 3-body modes are therefore expected and are taken into account, based on data in the true mode. Fig. 6 shows two Cabibbo-favored Ξ_c^+ modes decaying to $\Xi^-\pi^+\pi^+$ and $\Sigma^+K^-\pi^+$, respectively. For these modes, we require additional kinematical cuts: (a) the transverse component of the reconstructed parent particle momentum with respect to the line of flight less than 0.3 GeV, and (b) the momentum of the π^+ is greater than 10 GeV. The shaded area in $\Xi^-\pi^+\pi^+$ and $\Sigma^+K^-\pi^+$ is the estimated reflection from $\Lambda_c^+ \rightarrow \Sigma^-\pi^+\pi^+$ and $\Lambda_c^+ \rightarrow \Sigma^+K^-\pi^+$, respectively. The shape is determined by a Monte Carlo simulation and

the area is normalized to the observed number of signal events in the Λ_c^+ data.

To estimate the total acceptance for decay modes of interest, we embedded Monte Carlo charm decays events in data events. We generated charm events with an average transverse momentum $\langle p_T \rangle = 1.0$ GeV and longitudinal momentum spectrum as observed for the Ξ_c^+ data. Detector hits, including resolution and multiple Coulomb scattering smearing effects, produced by these embedded tracks were OR'd into the hit banks of the underlying data event. The new ensemble of hits was passed through the SELEX off-line reconstruction. The total acceptance of each mode was determined from the number of fitted signal events from the charmed particle mass spectrum.

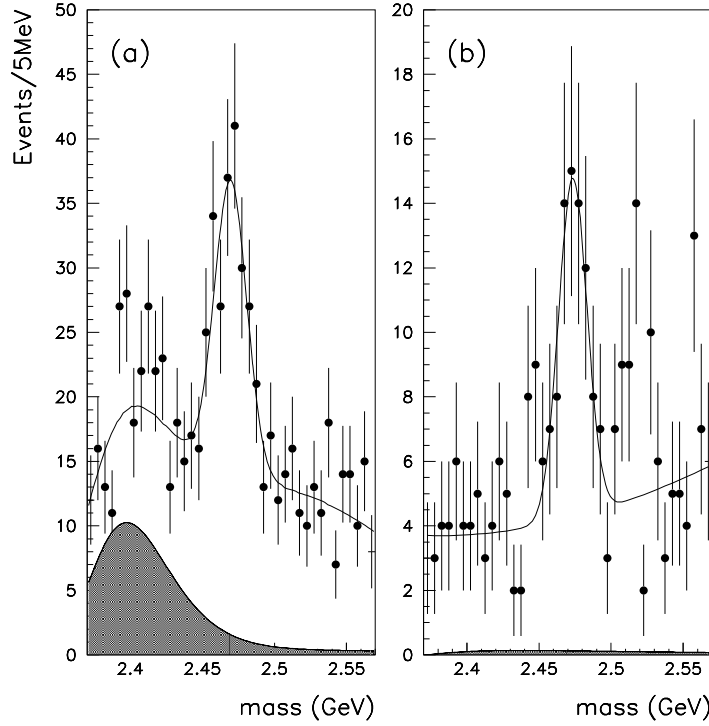


FIG. 6. Charmed baryon Ξ_c^+ signals with hyperon partial reconstruction, (a) $\Xi_c^+ \pi^+ \pi^+$ and (b) $\Xi_c^+ K^- \pi^-$.

To check the acceptance and particle identification, we measured two well-measured relative decay fractions, $B(D^0 \rightarrow K^- \pi^+ \pi^+ \pi^-)/B(D^0 \rightarrow K^- \pi^+) = 2.02 \pm 0.10 \pm 0.03$ and $B(D^+ \rightarrow K^- K^+ \pi^+)/B(D^+ \rightarrow K^- \pi^+ \pi^+) = 0.101 \pm 0.014 \pm 0.003$ where the first error is statistical and the second is the systematic difference between charge-conjugate states. The results agree well with the world averages [13]. For the D^+ decays, we applied a tighter cut $L/\sigma (> 12)$ to suppress background from $D_s^+ \rightarrow K^- K^+ \pi^+$ since the lifetime of D^+ is 2.4 times longer than that of D_s^+ .

To check the hyperon decay acceptance, we take into account two Cabibbo-favored modes $\Xi_c^+ \rightarrow \Sigma^+ K^- \pi^+$ and $\Xi_c^+ \rightarrow \Xi^- \pi^+ \pi^+$. We measure the relative branching fraction to be (1.12 ± 0.35) . The error is statistical only. This result is comparable to the CLEO measurement, $(1.18 \pm 0.26 \pm 0.17)$ [14]. The number of events and estimated acceptance for these three Ξ_c^+ modes with the same set of cuts are summarized in table I.

TABLE I. Summary of observed events and estimated acceptance for Ξ_c^+ modes.

	Acceptance(%)	Events
$\Xi_c^+ \rightarrow \Xi^- \pi^+ \pi^+$	1.61 ± 0.04	127 ± 24
$\Xi_c^+ \rightarrow \Sigma^+ K^- \pi^+$	0.59 ± 0.02	52 ± 13
$\Xi_c^+ \rightarrow p K^- \pi^+$	4.69 ± 0.06	85 ± 22

The preliminary branching fraction of the Cabibbo-suppressed decay $\Xi_c^+ \rightarrow pK^-\pi^+$ relative to the Cabibbo-favored $\Xi_c^+ \rightarrow \Sigma^+K^-\pi^+$ is measured to be 0.21 ± 0.07 which corresponds to $(4.0 \pm 1.3) \times \tan^2\theta_c$.

V. CONCLUSION

We observed a large production asymmetry in favour of Λ_c^+ over $\bar{\Lambda}_c^-$ for all three beams in the region $x_F \geq 0.3$. The asymmetry is stronger for baryon beams than for the π^- beam. We report the observation of the Cabibbo-suppressed decay $\Xi_c^+ \rightarrow pK^-\pi^+$ at mass = (2.467 ± 0.001) GeV with 162 ± 31 signal events. The relative branching fraction of the decay $\Xi_c^+ \rightarrow pK^-\pi^+$ to the Cabibbo-favored $\Xi_c^+ \rightarrow \Sigma^+K^-\pi^+$ is measured to be $B(\Xi_c^+ \rightarrow pK^-\pi^+)/B(\Xi_c^+ \rightarrow \Sigma^+K^-\pi^+) = 0.21 \pm 0.07$.

-
- [1] Carnegie Mellon University, Fermilab, University of Iowa, University of Rochester, University of Hawaii, University of Michigan-Flint, Petersburg Nuclear Physics Institute (Russia), Institute for Theoretical and Experimental Physics (Moscow), Institute for High Energy Physics (Protvino), Moscow State University, University of Sao Paulo, Centro Brasileiro de Pesquisas Fisicas, Universidade Federal de Paraiba, Insitute of High Energy Physics (Beijing), University of Bristol, Tel Aviv University, Max Planck Institut fuer Kernphysik (Heidelberg), University of Trieste and INFN, University of Rome and INFN, Universidad Autonoma de San Luis Potosi, Bogazici University
 - [2] P.Nason, S.Dawson and K.Ellis, Nucl. Phys.**B327**, 49 (1989).
 - [3] S.Frixione, M.L.Mangano, P.Nason, G.Ridolfi, Nucl. Phys.**B431**, 453 (1994).
 - [4] E769 Collaboration, G.A.Alves *et.al*, Phys. Rev. Lett.**72**, 812 (1994).
 - [5] E791 Collaboration, E.M.Aitala *et.al*, Phys. Lett.**B371**, 157 (1996).
 - [6] M. Baur, B. Stech and M. Wirbel, Z. Phys. **C34**, 103 (1987).
 - [7] CLEO Collaboration, C.P. Jessop *et al.*, Phys. Rev. Lett. **B423**, 56 (1994).
 - [8] E687 Collaboration, P.L. Frabetti *et al.*, Phys. Rev. Lett. **B314**, 477 (1993).
 - [9] J. Engelfried *et al.*, accepted for publication in Nucl. Instrum. Methods A. FERMILAB-PUB-98/299-E, hep-ex/9811001.
 - [10] WA89 Collaboration, M.I.Adamovich *et.al*, submitted to Eur. Phys. J. C., CERN-EP/98-41, hep-ex/9803021.
 - [11] H.-U. Bengtsson and T. Sjostrand, *Computer Physics Communications*, **82**, 74 (1994)
 - [12] J.G. Körner and M. Krämer, Z. Phys. C **55**, 659 (1992).
 - [13] Particle Data Group, C. Caso *et al.*, European Phys. Journal **C3**, 1 (1998).
 - [14] CLEO Collaboration, T. Bergfeld *et al.*, Phys. Lett. **B365**, 431 (1996).